

# Dependence of upwelling-mediated nutrient transport on wind forcing, bottom topography and stratification in the Gulf of Finland: model experiments

Jaan Laanemets<sup>1)</sup>, Victor Zhurbas<sup>1)2)</sup>, Jüri Elken<sup>1)</sup> and Emil Vahtera<sup>3)</sup>

<sup>1)</sup> Marine Systems Institute, Tallinn University of Technology, Akadeemia tee 21, Tallinn 12618, Estonia

<sup>2)</sup> Shirshov Institute of Oceanology, 36 Nakhimovsky Prospect, Moscow 117851, Russia

<sup>3)</sup> Finnish Institute of Marine Research, P.O. Box 2, FI-00561 Helsinki, Finland; current address: City of Helsinki, Environment Centre, P.O. Box 500, FI-00099 Helsinki, Finland

Received 18 Oct. 2007, accepted 15 Oct. 2008 (Editor in charge of this article: Timo Huttula)

Laanemets, J., Zhurbas, V., Elken, J. & Vahtera, E. 2009: Dependence of upwelling-mediated nutrient transport on wind forcing, bottom topography and stratification in the Gulf of Finland: Model experiments. *Boreal Env. Res.* 14: 213–225.

Numerical simulation experiments with an eddy-resolving ocean circulation model were performed to study nutrient transport to the surface layer by summer upwelling events in the Gulf of Finland. It is shown that upwelling along the southern coast of the Gulf, produced by easterly winds, brings more nutrients to the surface layer than upwelling along the northern coast produced by westerly winds of identical strength. The different ability of upwelling to transport nutrients to the surface layer along the southern and northern coasts is explained by features in the bottom topography. A steeper bottom slope and greater sea depth along the southern coast causes more nutrients to be transported to the surface layer. Offshore transport of upwelled nutrients is mostly caused by mesoscale structures — filaments and eddies. It is also shown that upwelling events along both coasts transport nutrients into the upper layer with a clear excess of phosphate. This phosphate excess might promote nitrogen-fixing cyanobacteria due to nitrogen limitation for other phytoplankton groups.

## Introduction

Blooms of nitrogen-fixing cyanobacteria (*Nodularia spumigena*, *Aphanizomenon* sp., *Anabaena* spp.) are common from the end of June to the end of August in the eutrophic and brackish Baltic Sea, including the Gulf of Finland (e.g. Finni *et al.* 2001). The occurrence of cyanobacteria blooms in the Baltic has been related to a low dissolved inorganic nitrogen (DIN) to dissolved inorganic phosphorus (DIP) ratio (e.g.

Niemi 1979, Laamanen and Kuosa 2005). A seasonal course of surface layer dissolved inorganic nutrient concentrations is observed, where nitrate and phosphate decline from winter maximum to summer minimum values (phosphate and nitrate concentrations below the detection level) preceding the annual blooms (e.g. HELCOM 2002). The bloom-forming and nitrogen-fixing cyanobacteria in the Baltic have generally high temperature requirements for efficient growth (Lehtimäki *et al.* 1997, Wasmund 1997). The growth-limiting nutrient for nitrogen-fixing cyanobacteria during

warm years is mainly phosphorus (Kangro *et al.* 2007) and bloom formation has been suggested to rely on different sources of phosphorus: intracellular storage of spring bloom excess phosphate, remineralisation of the upper layer phosphorus pool and phosphate input through turbulent mixing and upwelling (e.g. Kononen *et al.* 1996, Larsson *et al.* 2001, Lignell *et al.* 2003).

In summer when the water column is thermally stratified a coastal upwelling caused by transient along-shore wind forcing usually brings up cold and nutrient rich water. Satellite sea surface temperature (SST) data (e.g. Kahru *et al.* 1995) and model simulations (e.g. Myrberg and Andrejev 2003) showed that the northern coast of the Gulf of Finland is an active upwelling region in the Baltic Sea. Upwelling frequently results in the formation of filaments/squirts and eddies (e.g. Bychkova and Victorov 1988, Siegel *et al.* 1994, Kahru *et al.* 1995, Zhurbas *et al.* 2004) extending the domain of influence of upwelling from a narrow coastal zone into the basin interior. Numerical simulations by Zhurbas *et al.* (2008) showed that the relaxation of longshore baroclinic jets and related thermohaline fronts caused by coupled upwelling and downwelling events in the Gulf of Finland occurs in the form of cold and warm water filaments contributing to lateral mixing.

Analysis of nutrient data sampled in the western Gulf has revealed that the seasonal nutrient lines lie in the thermocline, the phosphocline being shallower than the nitracline (Laanemets *et al.* 2004). Thus, the vertical separation of the phosphocline and the nitracline may result in excess transport of phosphate into the surface layer, hypothetically favouring diazotrophic cyanobacteria. Field observations during an upwelling event along the northern coast of the Gulf, showed that upwelling brought mainly phosphate into the surface layer and that growth of cyanobacteria was promoted by the phosphate input with a three-week time lag (Vahtera *et al.* 2005). However, field observations during an upwelling event in a cold summer showed that the phosphate input may also prolong blooms of the migratory dinoflagellate *Heterocapsa triquetra* (Kononen *et al.* 2003). Compared with the Baltic Proper, the importance of phosphate input by summer upwelling events into the sur-

face layer may be emphasised in the Gulf of Finland because it is a narrow elongated basin experiencing frequent upwelling events.

The aim of the present paper is to evaluate total input of phosphate (phosphorus) and nitrate (nitrogen) by summer upwelling events to the surface layer and to map their distribution in the Gulf of Finland using results of model experiments. Applying the same initial nutrient and salinity fields, model simulations were performed with different wind forcing and upper layer temperatures.

## Model setup and validation

### Model setup

We apply the Princeton Ocean Model (POM) (Blumberg and Mellor 1983). The POM is a primitive equation, sigma coordinate, free surface, hydrostatic model with a 2.5 moment turbulent closure sub-model embedded. The model domain includes the whole Baltic Sea closed at the Danish straits; digital topography of the bottom is taken from Seifert and Kayser (1995). The horizontal step of the model grid is 0.5 nautical miles in the Gulf (*see* Fig. 1) and reaches 2 nautical miles in the rest of the Baltic Sea; there are 20  $\sigma$ -levels in the vertical direction. A model resolution of 0.5 nautical miles allows resolving mesoscale phenomena, including upwelling filaments/squirts (Zhurbas *et al.* 2008) controlled by the internal baroclinic Rossby radius which value varies within 2–5 km in the Gulf (e.g. Fennel *et al.* 1991, Alenius *et al.* 2003).

Model simulations were performed for a 20-day period starting on 20 July covering a field measurements period onboard r/v *Aranda*, Finnish Institute of Marine Research, (Fig. 1) from 20 to 29 July 1999 in the western Gulf of Finland (Vahtera *et al.* 2005). Wind stress and surface heat flux components for the simulation period were calculated from a gridded meteorological data set established and maintained at the Swedish Meteorological and Hydrological Institute (SMHI), the space and time resolution is 1° and 3 h, respectively. To calculate winds at 10-m level from the geostrophic wind vectors, the latter were turned counterclockwise by 15° and

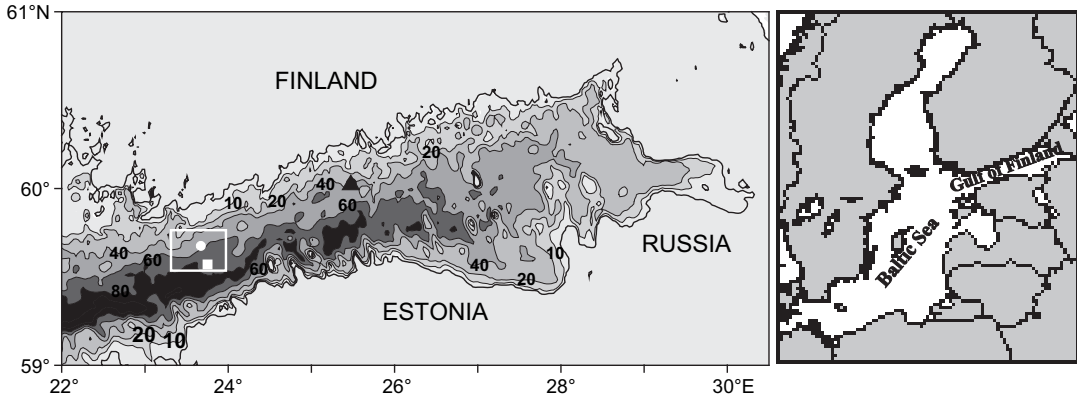


**Fig. 1.** Map of the Baltic Sea (right) and a close-up of the Gulf of Finland, where the model grid is refined to 0.5 nautical miles (left-hand side panel). Shown are the location of Kalbådagrund weather station ( $\blacktriangle$ ), *r/v Aranda* study area (within the rectangle), location of the fixed station (circle); and location of nutrient sampling used for construction of the initial field (square).

multiplied by a factor 0.6. Then 10-m-level wind components and other meteorological parameters were interpolated to the model grid. Since the surface winds calculated from the geostrophic gridded winds were too low as compared with the observations onboard the *r/v Aranda* and at the Kalbådagrund and Utö (59°46.8'N, 21°21.6'E) weather stations (Fig. 1), the gridded wind stress field ( $\tau$ ) was multiplied by a correction factor of 2.04, i.e. the corrected wind stress field is  $\tau_o = 2.04\tau$  (see Zhurbas *et al.* (2008) for more detail). The comparison of the corrected along-gulf wind stress component  $\tau_{ox}$  (positive eastward) with the wind stress component measured onboard *r/v Aranda* is presented in Fig. 2.

Initial thermohaline fields were constructed with the help of the Data Assimilation System (DAS) coupled with the Baltic Environmental Database (available at <http://nest.su.se/das>) using the climatological data from July to capture the main large-scale features of temperature and salinity. In the Gulf of Finland, long-term interpolation of upper mixed layer temperature on 20 July yielded values of approximately 16 °C (Fig. 3) versus approximately 19 °C measured on 20–21 July 1999 (Vahtera *et al.* 2005). Therefore, the initial temperature field constructed using DAS was increased by 3 °C in the upper 10-m layer of the whole Baltic Sea in order to fit the conditions of the specific year. Due to the smooth initial density field and weakness of related geostrophic currents, a windless model

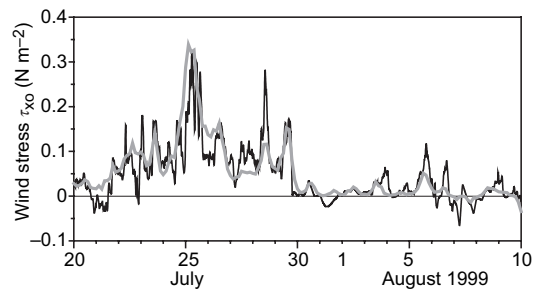


**Fig. 2.** Along-gulf components of wind stress for the period from 20 July to 9 August 1999 calculated from measurements at *r/v Aranda* (black, solid line) and from interpolations of the SMHI gridded meteorological data set (grey, solid line). Gaps in the *r/v Aranda* time series were filled with wind measurements at the Utö weather station.

adjustment period was not found necessary in order to study the wind-forced upwelling events, and we started model run from zero currents and sea level with wind forcing switched on. A justification for such an approach is that the Baltic currents respond to changing wind within approximately a day (Krauss and Brüggge 1991).

Two equations describing passive tracer balance were added to the POM and were used to simulate nutrient (phosphate and nitrate) transport. In order to estimate the total amount of nutrients transported from deep layers to the upper mixed layer, nutrients were considered as conservative passive tracers. Posterior behaviour of nutrients in the upper layer during the

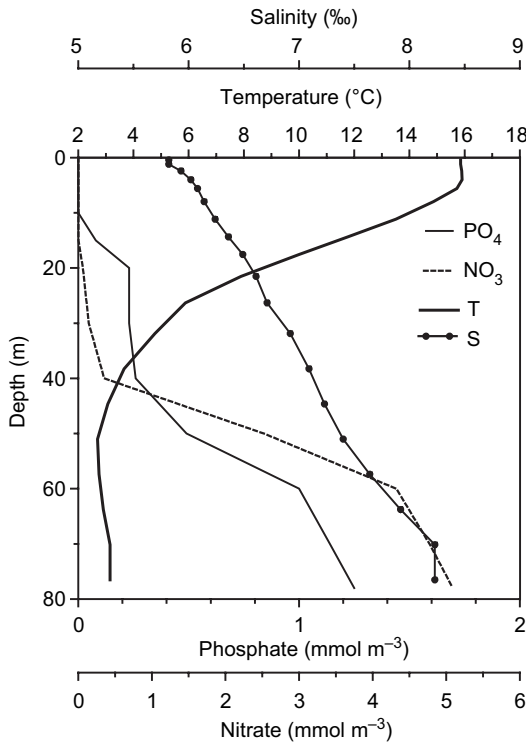


**Fig. 3.** Vertical profiles of phosphate and nitrate concentration measured on 20 July 1999 at sampling station ( $23^{\circ}40'E$ ,  $59^{\circ}32'N$ ) aboard *r/v Aranda*, temperature and salinity obtained by interpolation of DAS data to 20 July ( $23^{\circ}40'E$ ,  $59^{\circ}32'N$ ).

relaxation phase of upwelling is however not conservative, e.g. due to rapid phytoplankton uptake. Nevertheless, the simulated nutrient distributions may be used to display the role of filaments and eddies in the offshore transport of nutrients remaining in the surface layer after upwelling favourable winds cease. The equations were solved numerically within the POM code in the same way as those for temperature and salinity. For details of numerical integration of the equation for a scalar variable with the sigma coordinate system we refer the reader to Mellor and Blumberg (1985).

To construct initial fields of nutrients, we used data on phosphate and nitrate collected by *r/v Aranda* on 20 July 1999 in the open part of the western Gulf ( $59^{\circ}32'N$ ,  $23^{\circ}40'E$ ) (see Figs. 1 and 3). The vertical separation between the phosphocline and nitracline was about 5 m (Fig. 3), which is typical for summer nutriclines in the western Gulf (Laanemets *et al.* 2004). The maxi-

mum sampling depth was 60 m, and we extended the profiles to greater depths using the data from previous cruises. Vertical profiles of nutrients presented in Fig. 3 were uniformly extended to the whole Baltic Sea. The model runs from the motionless state and zero surface elevation at 00:00 a.m. of 20 July 1999.

## Model validation

The ability of the model to reproduce upwelling and its relaxation process, including upwelling filaments and eddies that are mostly associated with baroclinic instability, was proven in Zhurbas *et al.* (2008) based on comparisons of simulated SST maps with satellite SST images and field observations. In addition, for validation of the model performance it is worthwhile to compare the simulated time series of temperature, phosphate and nitrate concentrations in the upper mixed layer with corresponding measured values at a fixed station (Fig. 1) during *r/v Aranda* cruise in July 1999. Measurements at the fixed station ( $59^{\circ}42.5'N$ ,  $23^{\circ}37.8'E$ ) were carried out during two periods 22–23 and 25–27 July with the durations of 41 and 48 h, respectively (Vahtera *et al.* 2005). The first measurement period coincided with the start of the upwelling and the second one covered the well-developed phase of the upwelling; the fixed station was located in the upwelling front. CTD casts were performed at 1- to 2-h intervals and water samples for nutrient analyses were collected at 2- to 4-h intervals. The model has reproduced the temporal course of temperature reasonably well. The largest discrepancies between modelled and measured time series for temperature are likely caused by short-term/sub-grid variability of the upwelling front, which cannot be resolved properly by the model. During the first sampling period, the nitrate (phosphate) concentrations, both measured and simulated, were clearly (in almost all cases) below the detection limit (Fig. 4). By the second sampling period, after the culmination of the westerly winds on 25 July, the cold and nutrient-rich water covered the fixed station area which is clearly seen from both measured and simulated values. Taking into account the detection limit and the margin of error for the nutrient measure-

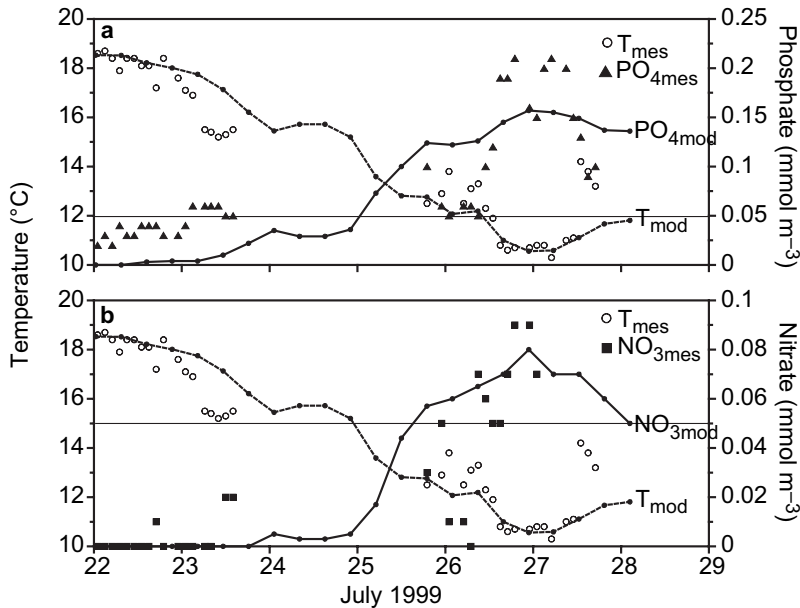


**Fig. 4.** Comparison of upper-layer simulated and measured temperature, phosphate and nitrate temporal course at the location of fixed station. Simulated parameters were stored at 6.96 h (half of the inertia oscillation period) intervals. **(a)** simulated temperature (dashed curve with dots) and phosphate (curve with dots), measured temperature (circles) and phosphate (filled triangles). **(b)** simulated temperature (dashed curve with dots) and nitrate (curve with dots), measured temperature (circles) and nitrate (filled triangles). The detection limit for both phosphate and nitrate is  $0.05 \text{ mmol m}^{-3}$  and is shown with a thin, horizontal line. The margins of error for the nutrient measurements are: for phosphate 35% at concentrations less than  $0.25 \text{ mmol m}^{-3}$  and 19% otherwise, for nitrate 23% at concentrations less than  $0.25 \text{ mmol m}^{-3}$  and 13% otherwise.

ments (*see* legend to Fig. 4), we may assert that the course of both phosphate and nitrate concentrations associated with upwelling event are reasonably well reproduced by the model.

## Results of model simulations

### Dependence of nutrient transport on wind forcing, bottom topography, and temperature stratification

To investigate how nutrient transport into the upper mixed layer depends on wind forcing, model experiments were performed with wind forcing of 0.25, 0.5, 1.0 and 1.5 times the corrected wind stress  $\tau_0$ . The reverse wind stress ( $-0.25\tau_0$ ,  $-0.5\tau_0$ ,  $-1.0\tau_0$  and  $-1.5\tau_0$ ) was applied to investigate the nutrient transport by upwelling along the southern coast of Gulf, which is characterized by a steep bottom topography and larger sea depth (*see* Fig. 1). For all simulations the same initial nutrient, salinity, and tempera-

ture (the upper layer temperature of  $19^\circ\text{C}$ ) fields were used.

To evaluate the total nutrient input by an upwelling event the content of nutrients in the upper 10-m layer was calculated by integrating over the whole Gulf area. The longitude  $23^\circ\text{E}$  is treated as the western boundary of the Gulf of Finland basin in the present study. The chosen depth of the upper mixed layer approximately corresponds to the depth of the euphotic zone, the depth where surface light intensity falls to 1% of that of the surface. In the relatively turbid Gulf of Finland the depth of the euphotic zone is about 10 m (e.g. Kononen *et al.* 2003).

Temporal courses of total content of phosphate phosphorus ( $\text{PO}_4\text{-P}$ ) and nitrate nitrogen ( $\text{NO}_3\text{-N}$ ) in the upper 10-m layer of the Gulf corresponding to the 8 different wind forcing regimes are depicted in Fig. 5. Transport of both phosphate and nitrate into the upper layer was remarkably larger in the southern (where the bottom slope is much steeper) than in the northern coastal sea area for all wind forcing magnitudes

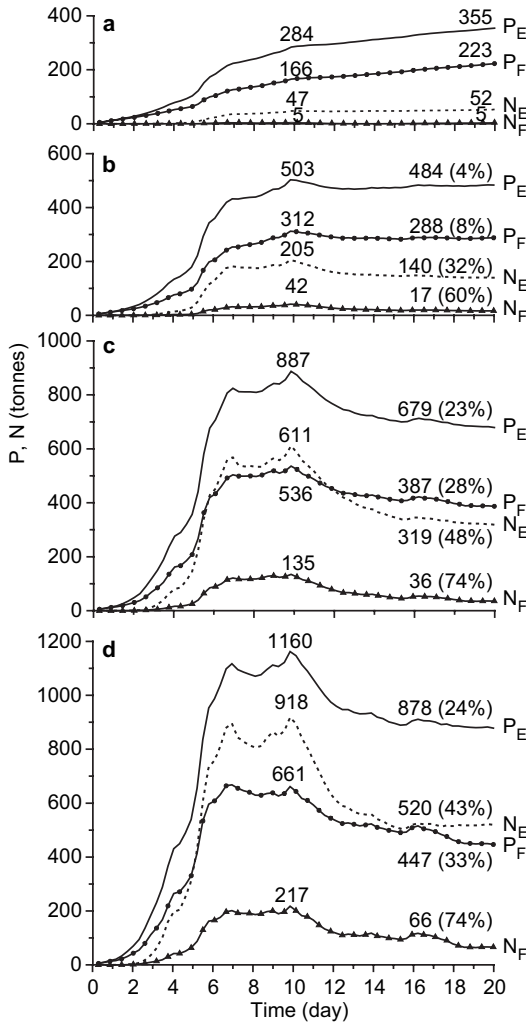


**Fig. 5.** Time series of total content of  $\text{PO}_4\text{-P}$  (P) and  $\text{NO}_3\text{-N}$  (N) introduced to the upper 10 m layer due to upwelling events caused by different wind forcing in the Gulf of Finland. The initial upper layer temperature was  $19^\circ\text{C}$  in all model experiment runs. Upwelling along the Finnish coast: P: solid line with dots, N: solid line with triangles. Upwelling along the Estonian coast: P: solid line, N: dashed line. (a) model runs with wind stress  $0.25\tau_0$  and  $-0.25\tau_0$ . (b) model runs with wind stress  $0.5\tau_0$  and  $-0.5\tau_0$ . (c) model runs with wind stress  $1.0\tau_0$  and  $-1.0\tau_0$ . (d) model runs with wind stress  $1.5\tau_0$  and  $-1.5\tau_0$ . The numbers above the curves show maximum contents of P and N (tonnes) and those at the end of simulations. Percentage decrease of P and N contents during relaxation of upwelling are given in parentheses.

applied. Since the nitracline is situated deeper than the phosphocline, nitrate transport into the upper layer during the course of an upwelling event begins later than that of phosphate. The

increase of nitrate content was also faster in the case of upwelling along the southern coast. The upper-layer content of nutrients reached maximum values by the time when upwelling promoting winds died down at  $t = 9.84$  days. The exception is in the case of weak wind forcing  $|t| = 0.25|\tau_0|$  when the nutrient contents were relatively low and grew even after the winds ceased, likely due to vertical turbulent diffusion.

Nitrogen transport by the upwelling along the northern coast was minor, maximum estimated values were from 5 to 217 tonnes. During the relaxation phase, starting from the 10th day of simulations (30 July, Fig. 2) the content of nitrogen in the upper layer decreased remarkably, up to 74% from maximum value in the surface layer due to sinking of upwelled cold and dense water. The phosphorus transport was larger, ranging from 166 to 661 tonnes depending on the wind forcing, and the relative decrease of total content in the upper layer by the end of simulation was smaller than for nitrogen (up to 33%).

Upwelling events along the southern coast transported remarkably larger amounts of nitrogen (from 47 to 918 tonnes) and phosphorus (from 284 to 1160 tonnes) into the surface layer in relation to those of the northern coast. Moreover, out-flow of nitrogen and phosphorus from the upper layer due to sinking of upwelled water was smaller (up to 48% and 24%, respectively, versus 74% and 33% along the northern coast).

Maps of phosphate and nitrate concentrations in the surface layer (at 1-m depth) for upwelling events along both coasts are presented in Figs. 6 and 7. Selected simulation times, 9.84 and 14.76 days, correspond to the maximum of nutrient input and to the time when out-flow of nutrients from the upper layer had almost ceased, respectively. The evident difference is that upwelling events along the southern coast bring more nutrients to the surface layer and cover larger areas by nutrient-rich upwelled water along the coastline (left panels in Figs. 6 and 7). It is clearly seen from the nutrient concentration maps, that transport of upwelled nutrients from the coastal zone to the open sea is mainly caused by mesoscale disturbances of the longshore upwelling front/jet in the shape of filaments and eddies.

To investigate how nutrient transport into the upper layer caused by upwelling depends on

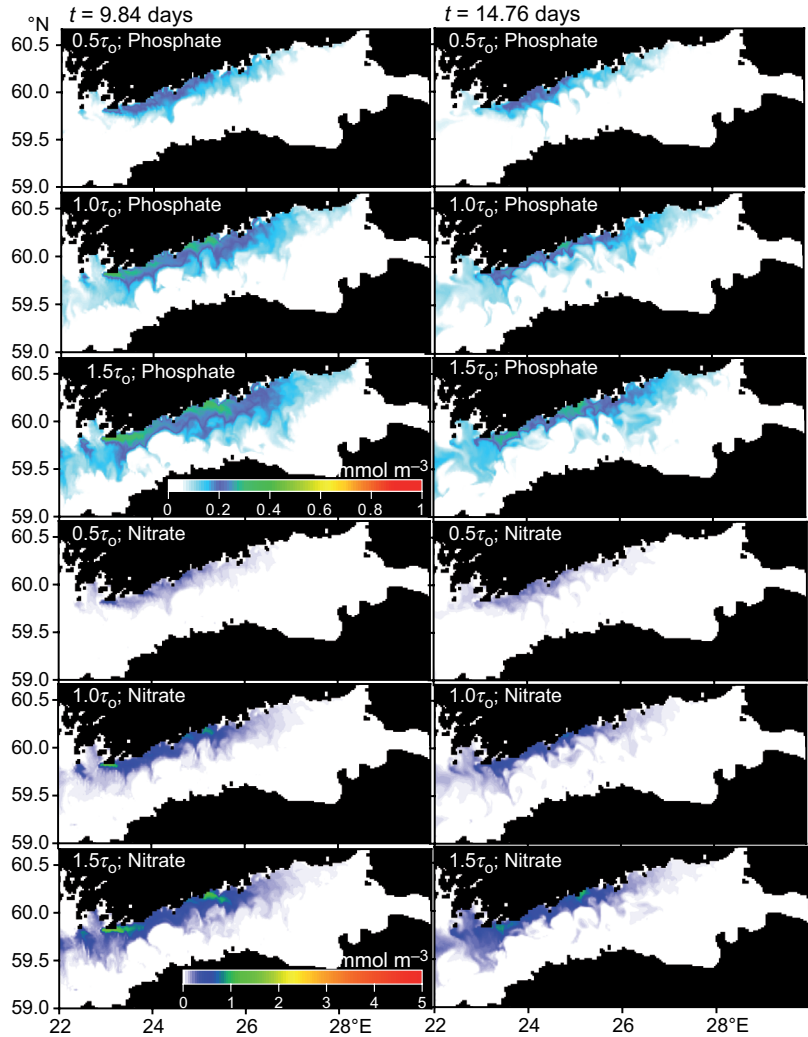


**Fig. 6.** Maps of phosphate (left panels) and nitrate (right panels) distributions in the upper layer at  $t = 9.86$  and  $14.76$  days. The initial surface layer temperature was set  $19\text{ }^{\circ}\text{C}$  and wind stresses  $0.5\tau_0$ ,  $1.0\tau_0$  and  $1.5\tau_0$  favourable for upwelling along the Finnish coast were applied. Separate colour scales for phosphate and nitrate were used.

thermocline strength, model simulations were performed for upper layer temperatures of  $16$ ,  $19$  and  $22\text{ }^{\circ}\text{C}$ . The upper layer temperature of  $16\text{ }^{\circ}\text{C}$  corresponds to cold and  $22\text{ }^{\circ}\text{C}$  to warm summers in the Gulf (e.g. Kononen *et al.* 2003, Laanemets *et al.* 2006).

Temporal courses of total content of phosphorus and nitrogen in the upper 10-m layer, corresponding to the three types of initial stratification situations, are depicted in Fig. 8. In the case of upwelling along the northern coast, an increase of thermocline strength resulted in some decrease of the maximum values in the temporal courses of total nutrient content, while, in the case of upwelling along the southern coast the concentrations remain practically unchanged. In

any case the changes in total nutrient content caused by changes of the upper layer temperature do not exceed 20%.

### Role of upwelling as a source of phosphate

To evaluate the importance of phosphorus inputs by summer upwelling events we compare the estimated inputs with estimates of monthly bio-available external loads of phosphorus to the Gulf of Finland. Annual total waterborne loads of phosphorus to the Gulf of Finland have been estimated to be up to 6030 tonnes, including phosphate phosphorus and organic phospho-

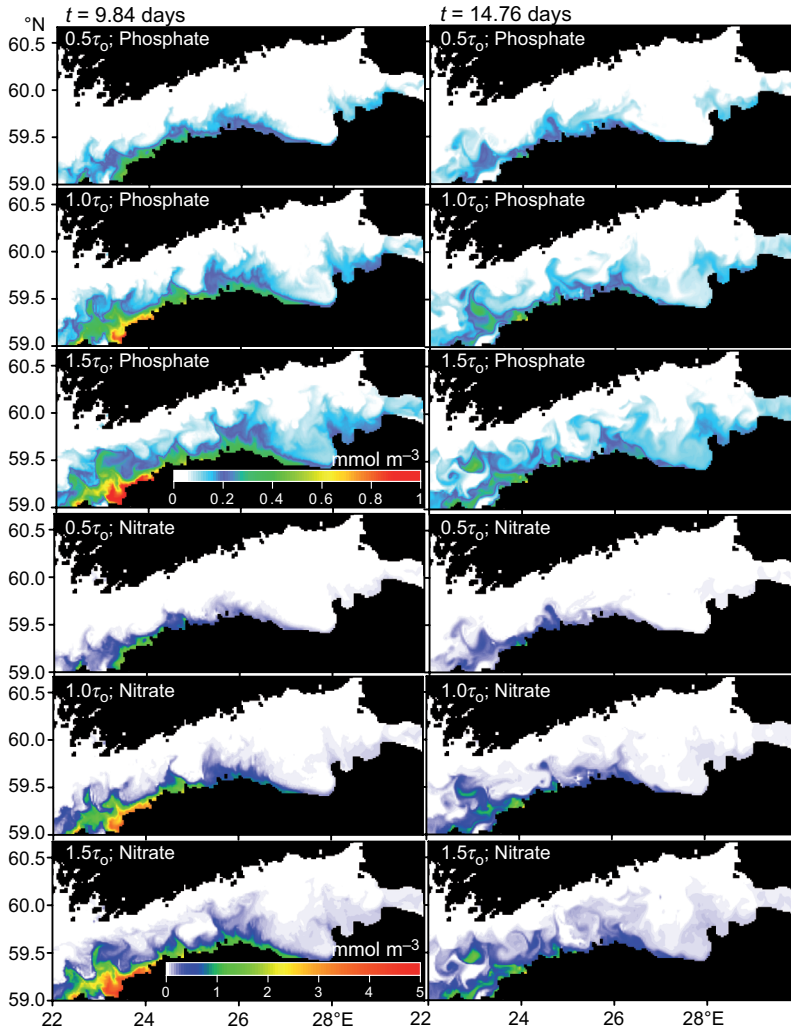


**Fig. 7.** Same as in Fig. 6 but for wind stresses  $-0.5\tau_0$ ,  $-1.0\tau_0$  and  $-1.5\tau_0$  favourable for upwelling along the Estonian coast.

rus compounds approximately in equal shares HELCOM (2004). The proportion of bioavailable organic phosphorus compounds varies within a large range. Nausch and Nausch (2006) estimated 8%–65% of organic phosphorus compounds to be bioavailable in the Baltic Proper pelagic areas. If we make an approximate estimation that half of the organic phosphorus compounds would be bioavailable, then the monthly external phosphorus load would reach values of 380 tonnes. Since external loads are to a large extent correlated with river runoff (e.g. Grimvall and Stålnacke 2001) it can be assumed that this number is rather overestimated since river runoff is small during late summer (Richter and Ebel 2006).

The amount of phosphorus remaining in the upper layer after relaxation of upwelling along the southern coast, even for weak wind forcing, were comparable and in the cases of stronger winds clearly exceeded the monthly external load of 380 tonnes (Fig. 5). Regardless of smaller amounts of phosphorus remaining in the upper layer after relaxation of upwelling along the northern coast, depending on wind forcing, 223–447 tonnes of phosphorus was brought to the surface layer.

Calculated total nutrient inputs to the upper layer were with clear excess of phosphorus. To illustrate the excess of phosphate in the upwelled water along the both coasts, we prepared maps of the nitrate/phosphate ratio for wind forcing

1.0 and  $1.5\tau_0$  at  $t = 9.84$  days (Fig. 9). Distributions of the nitrate/phosphate ratio displayed very low values, even in the narrow coastal zone where the nitrate concentrations were the highest (Figs. 6 and 7) the ratio remained below 5, much smaller than the Redfield ratio of 16 traditionally used to depict the nutrient demand ratio of rapidly growing phytoplankton (Sterner and Elser 2002). When the upwelling promoting wind dies down the ratio decreased due to the larger outflow of nitrate from the upper layer due to sinking of cold and dense water.

The clear excess of phosphate in the upwelled water displayed by all simulated scenarios suggests that a large part of the phosphate remaining in the upper layer after relaxation might be utilized by nitrogen-fixing cyanobacteria due to nitrogen limitation of other phytoplankton groups (Kangro *et al.* 2007). Besides this, Kononen *et al.* (2003) showed that phosphate input by upwelling may promote development of deep chlorophyll maxima of migratory dinoflagellates such as *H. triquetra* during cold summers.

## Discussion and conclusions

The above described results of model experiments display a striking feature of wind-driven upwelling events in the Gulf of Finland. Upwelling along the southern coast produced by easterly winds brings much more nutrients to the surface layer than upwelling along the northern coast produced by westerly winds of identical strength. The different ability to transport nutrients displayed by upwelling events along the southern and northern coasts is most pronounced

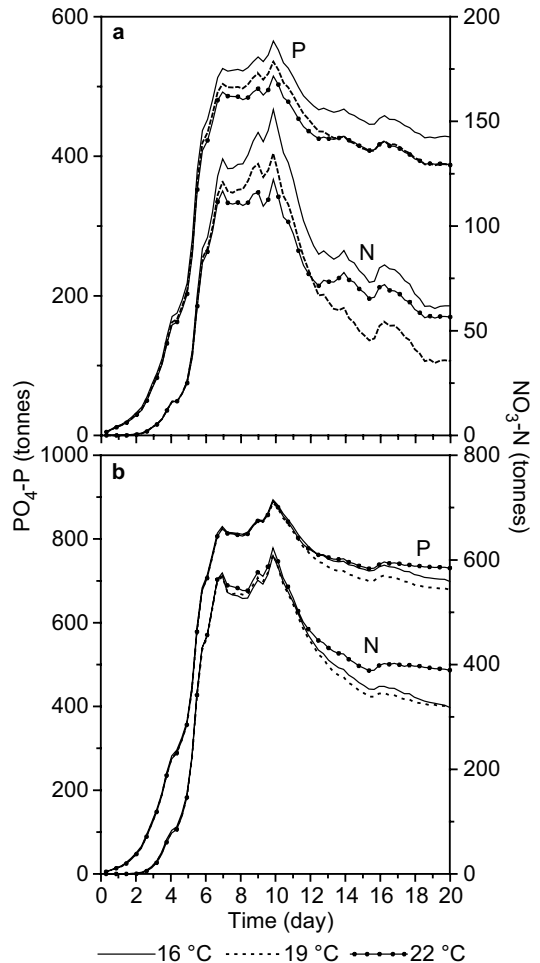


**Fig. 8.** Time series of simulated total content of  $\text{PO}_4\text{-P}$  (P) and  $\text{NO}_3\text{-N}$  (N) introduced to the upper 10 m layer due to upwelling events in the cases of different stratification. The upper layer temperature was set  $16^\circ\text{C}$  (P, N: solid),  $19^\circ\text{C}$  (P, N: dashed line) and  $22^\circ\text{C}$  (P, N: solid line with dots). (a) upwelling along the Finnish coast, wind stress  $\tau_0$ . (b) upwelling along the Estonian coast, wind stress  $-\tau_0$ .

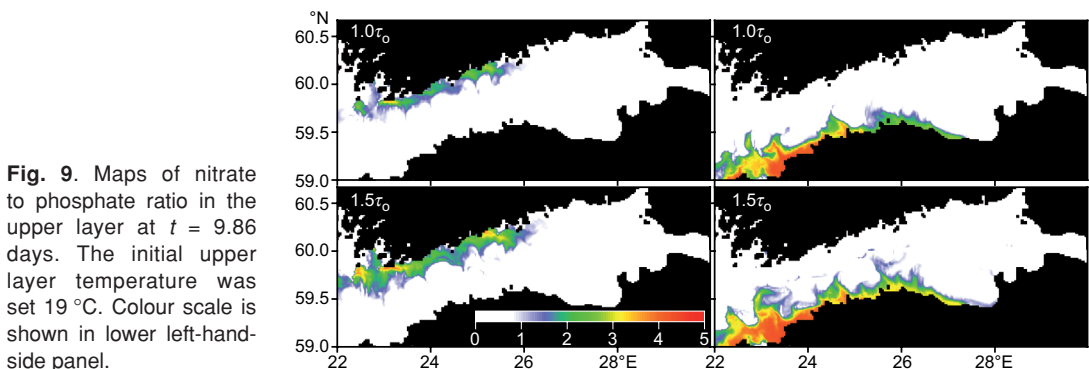


**Fig. 9.** Maps of nitrate to phosphate ratio in the upper layer at  $t = 9.86$  days. The initial upper layer temperature was set  $19^\circ\text{C}$ . Colour scale is shown in lower left-hand-side panel.

in the case of nitrate. The ratio of the maximum (residual after relaxation) values of respective nitrate inputs varied within 4.2–9.4 (7.9–10.4) (*see* Fig. 5). In the case of phosphate, the ratio is smaller but still considerably above unity, 1.6–1.8 (1.7–2.0). It seems worthwhile to discuss possible reasons, which may be responsible for the above mentioned differences.

Since the undisturbed concentrations of nutrients increase with depth (*see* Fig. 3), the amount of upwelled nutrients will depend on the vertical position of the onshore return flow that balances the offshore Ekman transport in the surface layer in the course of an upwelling event. Lentz and Chapman (2004) showed that the vertical position of the onshore return flow is controlled by the Burger number  $s = \alpha N/f$ , where  $\alpha$  is the bottom slope,  $N$  is the buoyancy frequency, and  $f$  is the Coriolis parameter. For  $s \ll 1$  (weak stratification and/or gentle bottom slope) the bottom stress balances the wind stress, and the onshore return flow is primarily in the inclined bottom boundary layer. For  $s \approx 1$  or larger (strong stratification and/or steep bottom slope), the nonlinear cross-shelf momentum flux divergence due to wind-driven cross-shelf circulation acting on the vertically sheared geostrophic alongshelf flow, balances the wind stress, the bottom stress is small, and the onshore return flow is in the interior and shifts to just below the surface boundary layer for  $s \approx 1.5$ –2.

Using temperature and salinity differences in the thermocline layer between 10-m and 50-m depths (Fig. 3), the buoyancy frequency is calculated at  $N = 0.025 \text{ s}^{-1}$ . The typical value of the bottom slope  $\alpha$  in the Gulf of Finland can be estimated at 0.002 and 0.004 for the northern and southern shores, respectively. Taking  $f = 0.000125 \text{ s}^{-1}$  and the above values for  $\alpha$  and  $N$ , we obtain  $s = 0.4$  and  $s = 0.8$  for upwelling events along the northern and southern shores, respectively. A priori we cannot decide whether  $s = 0.8$  relates to the  $s \ll 1$  or  $s \approx 1$  regimes. However, it is seen from Fig. 7 that the maximum value of phosphate and nitrate concentration simulated in the surface layer due to upwelling along the southern coast can be estimated at 1 and  $4.5 \text{ mmol m}^{-3}$ , respectively. Comparing these values with the undisturbed vertical profiles of nutrients (Fig. 3), we can conclude that

the onshore return flow related to upwelling along the southern coast originates from layers of approximately 60 m or deeper, which can be practically identified with the bottom boundary layer of the Gulf. Since the value of the bottom slope and Burger number for the northern coast are twice as small as those of the southern coast, the onshore return flow is in the bottom boundary layer whether it be upwelling along the northern or southern coasts.

To be delivered from a level  $H$  to the surface, a liquid particle containing nutrients should cover a distance  $H/\alpha$  within the inclined bottom layer, and nutrient concentration in the particle decrease during the course of delivery due to mixing with ambient waters. Therefore, the time required for a nutrient-containing liquid particle to reach the surface and the decrease of nutrient concentration in it will be roughly proportional to  $\alpha^{-1}$ .

The above simple consideration which, neglects transverse density gradients and pycnocline slopes due to the mean circulation (Andrejev *et al.* 2004), can explain why upwelling along the southern coast of the Gulf with relatively steep bottom topography brings much more nutrients to the surface layer than that of the northern coast, where the bottom slope is relatively gentle.

Features of bottom topography are likely also responsible for the smaller decrease of nutrient content of the surface layer during the post-upwelling relaxation period for the southern coast in relation to the northern coast (*see* numbers in Fig. 5). After upwelling promoting wind cease, surface layer nutrient content is maintained by the geostrophically balanced front separating cold upwelled waters from warm offshore waters. If the geostrophic balance is violated due to friction, the upwelling front will move towards the shore decreasing the upwelled water area and, therefore, decreasing total surface layer nutrient content. Due to steep bottom topography, the thickness of the water column under the upwelling front is larger and efficiency of bottom friction is smaller along the southern coast in comparison with the northern coast where the sea depth is shallower.

The above presented results demonstrated that an upwelling along the southern coast brought much more nutrients (phosphate) into

the upper layer compared with upwelling along the northern coast. Therefore, the net input of nutrients is largely determined by the frequency, strength and duration of westerly and easterly wind events during the warm season. A crucial point is also the depth and the vertical separation and strength of the pycnocline and nitracline that determines the amount and ratio of nutrients transported into the upper layer by upwelling. Besides physical factors, the formation of nutriclines depends on biogeochemical nutrient transformations, seasonal dynamics of phytoplankton biomass and species composition as well as inter-annual changes in external and internal loads.

The clear excess of phosphate in nutrient transport to the surface layer can be assumed to favour nitrogen-fixing cyanobacteria over other phytoplankton species (Niemi 1979, Kangro *et al.* 2007). The spatial distribution of the bloom biomasses of nitrogen fixing cyanobacteria is affected by wind induced advection (Kanoshina *et al.* 2003) and by the vertical transport of nutrients (Vahtera *et al.* 2005). However, these processes work on different temporal scales. The winds that induce upwelling events cause an instantaneous advection of already existing surface accumulations of cyanobacteria, along with the old surface water. Due to the positive buoyancy of bloom forming cyanobacteria this causes existing bloom biomasses to accumulate in frontal zones and on the downwelling side of the Gulf.

Phosphate inputs by upwelling events promote cyanobacteria blooms with a time lag of two to three weeks (Vahtera *et al.* 2005) therefore the timing and frequency of upwelling events are important when considering potential bloom promotion by upwelling events. Phosphate input by upwelling during early summer more likely promotes cyanobacteria blooms than phosphate inputs during the bloom peak. Phosphate excess introduced to the surface layer during early summer may be stored and used during the short time window with warm surface waters and high irradiance suitable for rapid cyanobacteria growth (Lehtimäki *et al.* 1997, Vahtera *et al.* 2007).

The northern shore of the Gulf is more frequently affected by upwelling due to dominant

westerly or south-westerly winds (Myrberg and Andrejev 2003). Therefore, during summers of frequent upwelling the northern shore of the Gulf might be less affected by pelagic cyanobacteria blooms due to flushing of the surface layer by deeper and colder waters with less cyanobacteria biomass and due to the fact that the cyanobacteria grow rather slowly even under optimal conditions (e.g. Vahtera *et al.* 2007). However, periods of weak westerly or south-westerly winds or reversed winds, cyanobacteria grow and accumulate also along the northern coast of the Gulf (Vahtera *et al.* 2005), as can be seen also in composite satellite images of cyanobacteria surface accumulations (Kahru *et al.* 2007).

The different ability of upwelling to transport phosphate to the surface layer along the northern and southern coasts might also affect the potential bloom promotion of upwelling in the Gulf. The notion that upwelling along the southern coast is less frequent and brings considerably more phosphate to the surface layer may render it more susceptible to bloom occurrence. Further studies are needed to quantify net phosphate and nitrate inputs by upwelling events to the surface layer along with studies on the timing and frequency of the events and the effect on the spatial and temporal distribution of cyanobacteria bloom biomasses.

*Acknowledgements:* We are thankful to anonymous reviewers for constructive recommendations. The work was sponsored by EU Structural Funds (ESF measure 1.1), the Estonian Science Foundation (Grant #7467 and #7328) and the Russian Foundation for Basic Research (Grant #09-05-00479). Finnish Meteorological Institute kindly provided weather station's wind data. Special thanks to Oleg Andrejev for provision of meteorological data.

## References

- Alenius P., Nekrasov A. & Myrberg K. 2003. Variability of the baroclinic Rossby radius in the Gulf of Finland. *Cont. Shelf. Res.* 23: 563–573.
- Andrejev O., Myrberg K., Alenius P. & Lundberg P.A. 2004. Mean circulation and water exchange in the Gulf of Finland — a study based on three-dimensional modelling. *Boreal Env. Res.* 9: 1–16.
- Blumberg A.F. & Mellor G.L. 1983. Diagnostic and prognostic numerical calculation studies of the South Atlantic Bight. *J. Geophys. Res.* 88: 4579–4592.
- Bychkova I.A. & Victorov S.V. 1988. Parameters of eddy

- structures and mushroom-shaped currents in the Baltic Sea from satellite images. *Issledovanie Zemli iz Kosmosa* 2: 29–35.
- Fennel W., Seifert T. & Kayser B. 1991. Rossby radii and phase speeds in the Baltic Sea. *Cont. Shelf Res.* 11: 23–36.
- Finni T., Kononen K., Olsonen R. & Wallstrom K. 2001. The history of cyanobacterial blooms in the Baltic Sea. *Ambio* 30: 172–178.
- Grimvall A. & Stålnacke P. 2001. Riverine inputs of nutrients to the Baltic Sea. In: Wulff F., Rahm L. & Larsson P. (eds.), *A systems analysis of the Baltic Sea*, Ecological Studies 148, Springer-Verlag, Berlin Heidelberg, pp. 113–128.
- HELCOM 2002. Environment of the Baltic Sea area 1994–1998. *Baltic Sea Environment Proceedings* 82B: 1–216.
- HELCOM 2004. The Fourth Baltic Sea Pollution Load Compilation (PLC-4). *Baltic Sea Environment Proceedings* 93: 1–188.
- Kahru M., Håkansson B. & Rud O. 1995. Distributions of the sea-surface temperature fronts in the Baltic Sea as derived from satellite imagery. *Cont. Shelf Res.* 15: 663–679.
- Kahru M., Savchuk O. & Elmgren R. 2007. Satellite measurements of cyanobacterial bloom frequency in the Baltic Sea: interannual and spatial variability. *Mar. Ecol. Prog. Ser.* 343: 15–23.
- Kangro K., Olli K., Tamminen T. & Lignell R. 2007. Species-specific responses of a cyanobacteria-dominated phytoplankton community to artificial nutrient limitation: a Baltic Sea coastal mesocosm study. *Mar. Ecol. Prog. Ser.* 336: 15–27.
- Kanoshina I., Lips U. & Leppänen J.-M. 2003. The influence of weather conditions (temperature and wind) on cyanobacterial bloom development in the Gulf of Finland (Baltic Sea). *Harmful Algae* 2: 29–41.
- Kononen K., Kuparinen J., Mäkelä K., Laanemets J., Pavelson J. & Nömmann S. 1996. Initiation of cyanobacterial blooms in a frontal region at the entrance to the Gulf of Finland, Baltic Sea. *Limnol. Oceanogr.* 41: 98–112.
- Kononen K., Huttunen M., Hällfors S., Gentien P., Lunven M., Huttula T., Laanemets J., Lilover M., Pavelson J. & Stips A. 2003. Development of a deep chlorophyll maximum of *Heterocapsa triquetra* Ehrenb. at the entrance to the Gulf of Finland. *Limnol. Oceanogr.* 48: 594–607.
- Krauss W. & Brüggge B. 1991. Wind-produced water exchange between the deep basins of the Baltic Sea. *J. Phys. Oceanogr.* 21: 373–394.
- Laamanen M. & Kuosa H. 2005. Annual variability of biomass and heterocysts of the  $N_2$ -fixing cyanobacterium *Aphanizomenon flos-aquae* in the Baltic Sea with reference to *Anabaena* spp. and *Nodularia spumigena*. *Boreal Env. Res.* 10: 19–30.
- Laanemets J., Kononen K., Pavelson J. & Poutanen E.L. 2004. Vertical location of seasonal nutriclines in the western Gulf of Finland. *J. Mar. Syst.* 52: 1–13.
- Laanemets J., Lilover M.-J., Raudsepp U., Autio R., Vahtera E., Lips I. & Lips U. 2006. A fuzzy logic model to describe the cyanobacteria *Nodularia spumigena* bloom in the Gulf of Finland, Baltic Sea. *Hydrobiologia*. 554: 31–45.
- Larsson U., Hajdu S., Walve J. & Elmgren R. 2001. Baltic Sea nitrogen fixation estimated from the summer increase in upper mixed layer total nitrogen. *Limnol. Oceanogr.* 46: 811–820.
- Lehtimäki J., Moisander P., Sivonen K. & Kononen K. 1997. Growth, nitrogen fixation, and nodularin production by two Baltic Sea cyanobacteria. *Appl. Environ. Microbiol.* 63: 1647–1656.
- Lentz S.J. & Chapman D.C. 2004. The importance of non-linear cross-shelf momentum flux during wind-driven coastal upwelling. *J. Phys. Oceanogr.* 34: 2444–2457.
- Lignell R., Seppälä J., Kuuppo P., Tamminen T., Andersen T. & Gismervik I. 2003. Beyond bulk properties: Responses of coastal summer plankton communities to nutrient enrichment in the northern Baltic Sea. *Limnol. Oceanogr.* 48: 189–209.
- Mellor G.L. & Blumberg A.F. 1985. Modeling vertical and horizontal diffusivities with the sigma coordinate system. *Monthly Weather Review* 113: 1380–1383.
- Myrberg K. & Andrejev O. 2003. Main upwelling regions in the Baltic Sea — a statistical analysis based on three-dimensional modeling. *Boreal Env. Res.* 8: 97–112.
- Nausch M. & Nausch G. 2006. Bioavailability of dissolved organic phosphorus in the Baltic Sea. *Mar. Ecol. Prog. Ser.* 321: 91–17.
- Niemi Å. 1979. Blue-green algal blooms and N:P ratio in the Baltic Sea. *Acta Bot. Fennica* 110: 57–61.
- Richter K.-G. & Ebel M. 2006. Analysis of runoff for the Baltic Sea basin with an integrated atmospheric–oceanic–hydrology model. *Advances in Geosciences* 9: 31–37.
- Seifert T. & Kayser B. 1995. *A high resolution spherical grid topography of the Baltic Sea*. Meereswissenschaftliche Berichte/Marine Science Reports, Institut für Ostseeforschung Warnemünde.
- Siegel H., Gerth M., Rudolph R. & Tschersich G. 1994. Dynamic features in the western Baltic Sea investigated using NOAA-AVHRR data. *Dt. Hydrogr. Z.* 46: 191–209.
- Sterner R.W. & Elser J.J. 2002. *Ecological stoichiometry: the biology of elements from molecules to the biosphere*. Princeton University Press, Princeton.
- Vahtera E., Laanemets J., Pavelson J., Huttunen M. & Kononen K. 2005. Effect of upwelling on the pelagic environment and bloom-forming cyanobacteria in the western Gulf of Finland, Baltic Sea. *J. Mar. Syst.* 58: 67–82.
- Vahtera E., Laamanen M. & Rintala J.-M. 2007. Use of different phosphorus sources by the bloom-forming cyanobacteria *Aphanizomenon flos-aquae* and *Nodularia spumigena*. *Aquat. Microb. Ecol.* 46: 225–237.
- Wasmund N. 1997. Occurrence of cyanobacterial blooms in the Baltic Sea in relation to environmental conditions. *Int. Revue ges Hydrobiol.* 82: 169–184.
- Zhubas V.M., Stipa T., Mälikki P., Paka V.T., Kuzmina N.P. & Sklyarov V.E. 2004. Mesoscale variability of upwelling in the southeastern Baltic Sea: Infrared images and numerical modeling. *Oceanology*. 44: 619–628.

Zhurbas V.M., Laanemets J. & Vahtera E. 2008. Modeling of the mesoscale structure of coupled upwelling/downwelling events and the related input of nutri-

ents to the upper mixed layer in the Gulf of Finland, Baltic Sea. *J. Geophys. Res.* 113: C05004, doi: 10.1029/2007JC004280.